

<https://doi.org/10.33472/AFJBS.6.9.2024.4972-4997>



African Journal of Biological Sciences

Journal homepage: <http://www.afjbs.com>



Research Paper

Open Access

Design and Synthesis of Benzimidazole Molecules Endowed with Hydrazine Carboxamides as Anticonvulsant agents

Bishmillah Azad^{a,*}, Anand Singh^a, Zulphikar Ali^b

^aSchool of Pharmaceutical Sciences, Dept. of Medical & Allied Sciences, Singhania University, Pachheri Bari, Jhunjhunu, Rajasthan, India.

^bAVIPS, Sobhit University, Gangoh, Saharanpur, UP, India.

Corresponding author: Bishmillah Azad

E-mail address: azadbismillah786@yahoo.co.in (Bishmillah Azad).

Tel. +91 9891940058; +91 8447846836

Article History

Volume 6, Issue 9, 2024

Received: 20 May 2024

Accepted : 15 Jun 2024

doi: 10.33472/AFJBS.6.9.2024.4972-4997

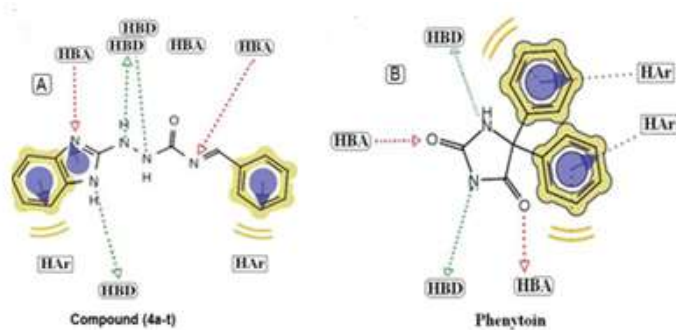
Abstract:

This work includes the design and synthesis of a class of carboxamides, designated (**4a-t**), of 1H-benzo[d]imidazol-2-yl)-N-benzylidene hydrazine derivatives. There were several steps involved in the synthesis technique, including pharmacophore modeling, *in vivo* screening, and investigating the binding mechanism of the produced compounds using molecular docking experiments performed using 3QEL protein, which is known to be an NMDA receptor antagonist. Most of the compounds showed anticonvulsant properties; based on maximal electroshock-induced seizures (MES), subcutaneous pentylenetetrazole (scPTZ), and an ED₅₀ of 19.3 mg/kg, compound (**4e**) (1-(1H-benzo[d]imidazol-2-yl)-N-(3-chlorobenzylidene) hydrazine carboxamide) was shown to be the most active among the series, free of neurotoxicity, even at the maximum dose of 300 mg/kg that was delivered. Enzymes, protein estimation, and ethanol potentiation were all carefully investigated to determine any possible negative effects on the liver, and it exhibits a favorable balance between potency and safety in the examined criteria, making it a viable lead for the creation of novel.

Key-words: Semicarbazones, Pharmacophore modeling, Molecular docking study, *In silico*, *In-vivo* anticonvulsant model.

Graphical abstract:

Molecular Design and Synthesis of Benzimidazole Derivatives as Emerging Anticonvulsant Agent



The title emphasizes most of the sources of the study parts, such as pharmacophore modeling, design, and synthesis of some benzimidazole derivatives and their in vivo evaluation for their anticonvulsant activity, while also insinuating the expected impact of the research and the upcoming installation of new anticonvulsant agents.

Introduction

Epilepsy has become a serious neurological disorder, and more than 50 million people are affected globally every year. It is characterized by chronic recurrent paroxysmal changes in neurologic function due to abnormalities in the electrical activity of the brain. Several patients who have seizures are resistant to the available medical therapies, or lifelong medication may be required. In addition to many available AEDs such as phenobarbital, phenytoin, trimethadione, primidone, carbamazepine, vigabatrin, valproate, felbamate, and lamotrigine which are effective in only 60-80% of patients but have reported undesirable effects such as headache, nausea, anorexia, ataxia, hepatotoxicity, drowsiness, gastrointestinal disturbance, gingival hyperplasia, and hirsutism.¹ The currently approved anticonvulsant agents have dose-related toxicity and idiosyncratic side effects². Therefore, there is a massive need for the development of novel AEDs

that are more selective toward the disease and have the minimum toxicity for the treatment. The synthesis of benzimidazole derivatives, with their diverse therapeutic properties, serves as a versatile scaffold for drug design and frequently interacts with crucial biological targets, exhibiting highly significant functions such as anticonvulsant, anticancer, antimicrobial, antiviral, anti-inflammatory, antiparasitic, and other properties.^{3-7, 27, 28.}

Pharmacophore modeling has been reported for antiepileptic activity owing to conformational investigations of prevailing agents such as phenytoin, carbamazepine, rufinamide, lamotrigine, and phenobarbitone.^{8, 9} The titled compounds embrace four pharmacophoric elements, which are essential for having anticonvulsant activity, as suggested by *Pandeya et al.*¹⁰ at meta and para positions; (ii) a hydrogen bonding domain [HBD]. (iii) Hydrogen bonding acceptor [HBA]; and (iv) another hydrophobic-hydrophilic site conveying pharmacokinetic property (Figure 1).

In this view, it generates pharmacophore hypotheses and identifies similar chemical features that are shared by a training set of well-known NR2B antagonisms. Most courier N-methyl-D-aspartate (NMDA) receptors have a binding mode, as does their interaction with ifenprodil-like noncompetitive ligands. Among pharmacophores, taking into consideration the significant structural information obtained from computational studies towards the NR2B subtype, the selective noncompetitive inhibitor (ligand) responsible for anticonvulsant activity. Motivated by these observations, it was thought worthwhile to prepare new compounds with benzimidazole ring systems in order to obtain promising anticonvulsant agents. Therefore, a series of benzimidazole moieties were synthesized and screened for their in-vivo anticonvulsant activity.

Materials and Methods:

Chemistry

The reagents and solvents utilized in the study were of laboratory reagent (LR) grade and sourced from reputable suppliers such as S.D. Fine Chemicals, E. Merck Ltd, and Sigma Aldrich.

Melting points were determined using open glass capillaries within a flask containing liquid paraffin, and the values are reported without correction. The progression of reactions was monitored through TLC plates (silica gel G) using two solvent systems: Toluene: Ethyl acetate: Formic acid (5:4:1, v/v) and Benzene: Acetone (9:1, v/v). Spot identification was achieved through exposure to iodine vapors or under UV-light. The characterization of synthetic compounds involved various analytical techniques. Fourier transform infrared (FT-IR) spectra were acquired in KBr pellets using a Jasco FT/IR 4100 spectrometer. Proton nuclear magnetic resonance ($^1\text{H-NMR}$) spectra were obtained on a Bruker 300 Ultra Shield (300MHz) spectrometer, with DMSO- d_6 as the solvent. Chemical shifts (δ) are reported in parts per million (ppm) relative to tetramethylsilane (TMS) used as an internal standard, and splitting pattern abbreviations were as follows: s (singlet), bs (broad singlet), d (doublet), dd (double doublet), t (triplet), m (multiplet). Mass spectra were recorded using LCMS/MS equipment, including Perkin Elmer and LABINDIA, Applied Bio-system with model number API 3000. Results are presented as m/z values. Elemental analyses were conducted using a PerkinElmer 240 analyzer, providing results within the range of $\pm 0.4\%$ for each analyzed element (C, H, N). These comprehensive analytical methods ensure a thorough characterization of the synthesized compounds.

The physicochemical data of synthetic scheme are illustrated in Table 1.

Synthesis of 1 H-benzo[d]imidazole-2-thiol (1)

Potassium hydroxide (1 mmol) and carbon disulfide (1 mmol) were introduced to commercially available o-phenylenediamine (1 mmol) in 10 mL of ethanol. The mixture was refluxed for 5-6 hours. Subsequently, Norit was added, and the reflux continued for an additional 15 minutes. After confirming the completion of the reaction through a single-spot TLC using solvent systems (toluene: ethyl acetate: formic acid, 5:4:1, or benzene: acetone, 9:1), the reaction mixture was cooled to room temperature. A solid mass precipitated, which was filtered and washed with excess water to eliminate the inorganic component. The obtained product was further purified by recrystallization with ethanol, yielding the pure compound (**1**)^{11, 12}. Solid powder; Yield: 78%; m.p.: 189-191°C, $R_f = 0.43$. FT-IR (KBr) ν_{\max} cm^{-1} : 3395 (N-H str.), 3051 (H-Ar str.), 2634 (S-H str). $^1\text{H-NMR}$ (DMSO- d_6 , 300MHz) δ (ppm): 12.31 (S-H), 10.93 (s, 1H, NH), 7.12-6.51 (m, 4H, Ar-H). $^{13}\text{C NMR}$ (DMSO- d_6): δ 151.93 (N=C-N), 130.72, 130.41, 127.68, 125.34, 116.58,

115.91 (Ar-C). ESI MS (m/z): 150 (M^+). Anal cal. for $C_7H_6N_2S$: C, 54.91; H, 4.37; N, 15.12. Found: C, 54.87; H, 4.39; N, 15.25.

Synthesis of 2-hydrazinyl-1H-benzo[d]imidazole (2)

Compound (1) (1 mmol) was dissolved in methanol (10 mL) to form a solution. Hydrazine hydrate (1 mmol) was added gradually to the reaction mixture, followed by refluxing for 2-3 hours. After confirming the completion of the reaction, the mixture was cooled to room temperature, diluted with cold water, resulting in the formation of a precipitate. The precipitate was filtered and then crystallized from ethanol, yielding compound (2) as a creamy white solid powder. Yield: 74%; m.p.: 224-225°C, Rf = 0.51. FT-IR (KBr) ν_{\max} cm^{-1} : 3464 (N-H str.), 3024 (H-Ar str.). 1H -NMR (DMSO- d_6 , 300MHz) δ (ppm): 6.69 (s, 1H, NH), 7.42-7.72 (m, 4H, Ar-H), 9.02 (s, 1H, NH, Ar-H, D_2O exchangeable). ^{13}C NMR (DMSO- d_6): δ 152.31 (N=C-N), 131.63, 129.51, 129.17, 123.81, 115.17, 114.95 (Ar-C). ESI MS (m/z): 148 (M^+). Anal cal. for $C_7H_8N_4$: C, 56.74; H, 5.44; N, 37.81. Found: C, 56.81; H, 5.43; N, 37.83.

Synthesis of 2-(1H-benzo[d]imidazol-2-yl) hydrazinecarboxamide (3)

A solution of sodium cyanate (5 mL) in the minimum amount of water and glacial acetic acid (5 mL) was heated with compound (2) (0.01 mmol) in alcohol until the mixture became turbid, and the volume reduced to half of its original volume. The resulting mixture was added to ice-cold water, leading to the formation of a turbid solid. After filtration, drying, and subsequent crystallization with ethanol, pure compound was obtained (3) as a yellowish solid powder; Yield: 71%; m.p.: 238-239°C, Rf = 0.55. FT-IR (KBr) ν_{\max} cm^{-1} : 3505 (N-H str.), 3028 (H-Ar str.), 1623 (C=O). 1H -NMR (DMSO- d_6 , 300MHz) δ (ppm): 6.78 (s, 1H, NH), 7.22-7.73 (m, 4H, Ar-H), 9.56 (s, 1H, NHC=O, D_2O exchangeable). ^{13}C NMR (DMSO- d_6): δ 163.73 (C=O), 155.61 (N=C-N), 130.52, 129.47, 128.99, 121.65, 113.43, 113.17 (Ar-C). ESI MS (m/z): 191 (M^+). Anal cal. for $C_8H_9N_5O$: C, 50.35; H, 5.41; N, 31.63. Found: C, 50.39; H, 5.45; N, 31.71.

General procedure for the synthesis of substituted (1H-benzo[d]imidazol-2-yl)-N-benzylidene hydrazinecarboxamides (4a-t)

To create a solution, compound (3) (1 mmol) was dissolved in glacial acetic acid (5 mL), and ethanol (10 mL) was added. The mixture was then heated to boiling. A specific aromatic aldehyde/ketone (0.112 mmol) was introduced, and the reaction was refluxed for 5 hours. Upon

confirming completion through a single-spot TLC using solvent systems (toluene: ethyl acetate: formic acid, 5:4:1, or benzene: acetone, 9:1), the reaction mixture was cooled to room temperature and left overnight. A solid mass precipitated, and it was subsequently filtered and washed with an excess of water to remove the inorganic component. The obtained product was re-crystallized with ethanol to yield the pure compound.

Synthesis of 2-(1H-benzo[d]imidazol-2-yl)-N-benzylidenehydrazine carboxamide (4a)

Yield: 70%. m.p.: 268-269°C. FT-IR (KBr) ν_{\max} cm^{-1} : 3489 (N-H str.), 3020 (H-Ar str.), 1794 (C=N str), 1685 (C=O). $^1\text{H-NMR}$ (DMSO- d_6 , 300MHz) δ (ppm): 6.75 (s, 1H, NH), 7.12-7.83 (m, 9H, Ar-H), 12.56 (s, 1H, NHC=O, D₂O exchangeable). $^{13}\text{C NMR}$ (DMSO- d_6): δ 169.51 (C=O), 157.63 (C-H), 153.46 (N=C-N), 132.53, 131.62, 129.47, 128.72, 128.21, 125.83, 125.17, 123.23, 120.41, 118.54, 117.61, 112.93 (Ar-C). ESI MS (m/z): 279 (M^+).

Synthesis of 2-(1H-benzo[d]imidazol-2-yl)-N-(2-hydroxybenzylidene) hydrazinecarboxamide (4b)

Yield: 60%. m.p.: 264-265°C. FT-IR (KBr) ν_{\max} cm^{-1} : 3495 (N-H str.), 3064 (H-Ar str.), 1694 (C=N str), 1675 (C=O). $^1\text{H-NMR}$ (DMSO- d_6 , 300MHz) δ (ppm): 5.56 (s, 1H, OH), 6.55 (s, 1H, NH), 7.02-7.66 (m, 8H, Ar-H), 12.67 (s, 1H, NHC=O, D₂O exchangeable).

Synthesis of 2-(1H-benzo[d]imidazol-2-yl)-N-(4-hydroxybenzylidene) hydrazinecarboxamide (4c)

Yield: 62%. m.p.: 238-239°C. FT-IR (KBr) ν_{\max} cm^{-1} : 3467 (N-H str.), 3064 (H-Ar str.), 1824 (C=N str), 1646 (C=O). $^1\text{H-NMR}$ (DMSO- d_6 , 300MHz) δ (ppm): 6.86 (s, 1H, NH), 7.16-7.78 (m, 8H, Ar-H), 9.42 (s, 1H, OH), 12.36 (s, 1H, NHC=O, D₂O exchangeable).

Synthesis of 2-(1H-benzo[d]imidazol-2-yl)-N-(2-chlorobenzylidene) hydrazinecarboxamide (4d)

Yield: 57%. m.p.: 266-267°C. FT-IR (KBr) ν_{\max} cm^{-1} : 3228 (N-H str.), 3033 (H-Ar str.), 1804 (C=N str), 1690 (C=O), 767 (C-Cl). $^1\text{H-NMR}$ (DMSO- d_6 , 300MHz) δ (ppm): 6.56 (s, 1H, NH), 7.18-7.77 (m, 8H, Ar-H), 11.26 (s, 1H, NHC=O, D₂O exchangeable).

Synthesis of 2-(1H-benzo[d]imidazol-2-yl)-N-(4-chlorobenzylidene) hydrazinecarboxamide (4e)

Yield: 62%. m.p.: 276-277°C. FT-IR (KBr) ν_{\max} cm^{-1} : 3358 (N-H str.), 3033 (H-Ar str.), 1804 (C=N str), 1690 (C=O), 764 (C-Cl). $^1\text{H-NMR}$ (DMSO- d_6 , 300MHz) δ (ppm): 5.98 (s, 1H, NH),

7.11-7.69 (m, 8H, Ar-H); 12.68 (s, 1H, NHC=O, D₂O exchangeable). ¹³C NMR (DMSO-*d*₆): δ 167.43 (C=O), 161.89 (C-H), 154.71 (N=C-N), 134.51, 131.81, 131.23, 127.53, 126.21, 125.32, 124.35, 122.15, 121.68, 116.43, 115.72, 113.56 (Ar-C). ESI MS (*m/z*): 313 (M⁺).

Synthesis of 2-(1H-benzo[d]imidazol-2-yl)-N-(2-nitrobenzylidene) hydrazinecarboxamide (4f)
Yield: 66%. m.p.: 267-268°C. FT-IR (KBr) ν_{max} cm⁻¹: 3408 (N-H str.), 3063 (H-Ar str.), 1823 (C=N str), 1674 (C=O), 1337 (NO₂). ¹H-NMR (DMSO-*d*₆, 300MHz) δ (*ppm*): 6.25 (s, 1H, NH), 7.8-7.98 (m, 8H, Ar-H); 12.12 (s, 1H, NHC=O, D₂O exchangeable).

Synthesis of 2-(1H-benzo[d]imidazol-2-yl)-N-(4-nitrobenzylidene) hydrazinecarboxamide (4g)
Yield: 65%. m.p.: 258-259°C. FT-IR (KBr) ν_{max} cm⁻¹: 3438 (N-H str.), 3043 (H-Ar str.), 1784 (C=N str), 1666 (C=O), 1367 (NO₂). ¹H-NMR (DMSO-*d*₆, 300MHz) δ (*ppm*): 6.57 (s, 1H, NH), 7.16-8.33 (m, 8H, Ar-H); 11.14 (s, 1H, NHC=O, D₂O exchangeable).

Synthesis of 2-(1H-benzo[d]imidazol-2-yl)-N-(2-methoxybenzylidene) hydrazinecarboxamide (4h)
Yield: 61%. m.p.: 245-246°C. FT-IR (KBr) ν_{max} cm⁻¹: 3398 (N-H str.), 3083 (H-Ar str.), 1644 (C=N str); 1635 (C=O); 1598 (N=C-N). ¹H-NMR (DMSO-*d*₆, 300MHz) δ (*ppm*): 3.56 (s, 3H, OCH₃), 6.57 (s, 1H, NH), 7.16-8.33 (m, 8H, Ar-H); 11.14 (s, 1H, NHC=O, D₂O exchangeable). ¹³C NMR (DMSO-*d*₆): δ 168.23 (C=O), 155.71 (C-H), 153.47 (N=C-N), 143.65, 132.21, 131.84, 128.31, 125.45, 124.26, 120.13, 119.71, 119.15, 115.83, 115.01, 112.32 (Ar-C). ESI MS (*m/z*): 324 (M⁺).

Synthesis of 2-(1H-benzo[d]imidazol-2-yl)-N-(3,4-dimethoxybenzylidene) hydrazinecarboxamide (4i)
Yield: 62%. m.p.: 276-277°C. FT-IR (KBr) ν_{max} cm⁻¹: 3315 (N-H str.), 3096 (H-Ar str.), 1635 (C=O), 1623 (C=N str). ¹H-NMR (DMSO-*d*₆, 300MHz) δ (*ppm*): 3.53 (s, 3H, OCH₃), 3.83 (s, 3H, OCH₃) 5.27 (s, 1H, NH), 7.2-7.48 (m, 7H, Ar-H); 12.05 (s, 1H, NHC=O, D₂O exchangeable).

Synthesis of (E)-2-(1H-benzo[d]imidazol-2-yl)-N-(4-(dimethylamino) benzylidene) hydrazinecarboxamide (4j)
Yield: 62%. m.p.: 274-275°C. FT-IR (KBr) ν_{max} cm⁻¹: 3395 (N-H str.), 3035 (H-Ar str.), 1844 (C=N str); 1653 (C=O). ¹H-NMR (DMSO-*d*₆, 300MHz) δ (*ppm*): 2.97 (s, 3H, CH₃), 6.47 (s, 1H, NH), 7.12-7.50 (m, 8H, Ar-H); 11.75 (s, 1H, NHC=O, D₂O exchangeable).

Synthesis of 2-(1H-benzo[d]imidazol-2-yl)-N-(1-phenylethylidene) hydrazinecarboxamide (4k)

Yield: 74%. m.p.: 278-279°C. FT-IR (KBr) ν_{\max} cm^{-1} : 3489 (N-H str.), 3020 (H-Ar str.), 1794 (C=N str); 1685 (C=O). $^1\text{H-NMR}$ (DMSO- d_6 , 300MHz) δ (ppm): 1.85 (s, 3H, CH₃), 6.75 (s, 1H, NH), 7.12-7.83 (m, 9H, Ar-H); 12.56 (s, 1H, NHC=O, D₂O exchangeable).

Synthesis of (E)-2-(1H-benzo[d]imidazol-2-yl)-N-(1-(2-hydroxyphenyl) ethylidene)hydrazinecarboxamide (4l) Yield: 85%. m.p.: 240-241°C. FT-IR (KBr) ν_{\max} cm^{-1} : 3495 (N-H str.), 3064 (H-Ar str.), 1694 (C=N str), 1675 (C=O). $^1\text{H-NMR}$ (DMSO- d_6 , 300MHz) δ (ppm): 1.85 (s, 3H, CH₃), 6.57 (s, 1H, NH), 5.56 (s, 1H, OH) 7.02-7.66 (m, 8H, Ar-H); 12.67 (s, 1H, NHC=O, D₂O exchangeable).

Synthesis of (E)-2-(1H-benzo[d]imidazol-2-yl)-N-(1-(4-hydroxyphenyl) ethylidene)hydrazinecarboxamide (4m) Yield: 82%. m.p.: 256-257°C. FT-IR (KBr) ν_{\max} cm^{-1} : 3465 (N-H str.), 3023 (H-Ar str.), 1674 (C=N str), 1668 (C=O). $^1\text{H-NMR}$ (DMSO- d_6 , 300MHz) δ (ppm): 1.85 (s, 3H, CH₃), 5.68 (s, 1H, OH), 6.46 (s, 1H, NH), 7.22-7.76 (m, 8H, Ar-H); 12.58 (s, 1H, NHC=O, D₂O exchangeable).

Synthesis of 2-(1H-benzo[d]imidazol-2-yl)-N-(1-(2-chlorophenyl) ethylidene) hydrazinecarboxamide (4n) Yield: 78%. m.p.: 241-242°C. FT-IR (KBr) ν_{\max} cm^{-1} : 3436 (N-H str.), 3066 (H-Ar str.), 1812 (C=N str), 1684 (C=O). $^1\text{H-NMR}$ (DMSO- d_6 , 300MHz) δ (ppm): 2.02 (s, 3H, CH₃), 6.67 (s, 1H, NH), 7.03-7.77 (m, 8H, Ar-H); 11.43 (s, 1H, NHC=O, D₂O exchangeable).

Synthesis of 2-(1H-benzo[d]imidazol-2-yl)-N-(1-(4-chlorophenyl) ethylidene) hydrazinecarboxamide (4o) Yield: 81%. m.p.: 215-216°C. FT-IR (KBr) ν_{\max} cm^{-1} : 3512 (N-H str.), 3112 (CH-Ar str.), 1712 (C=N str) 1674 (C=O). $^1\text{H-NMR}$ (DMSO- d_6 , 300MHz) δ (ppm): 1.96 (s, 3H, CH₃), 5.93 (s, 1H, NH), 7.21-7.46 (m, 8H, Ar-H), 12.13 (s, 1H, NHC=O, D₂O exchangeable).

Synthesis of 2-(1H-benzo[d]imidazol-2-yl)-N-(1-(2-nitrophenyl) ethylidene)hydrazinecarboxamide (4p) Yield: 79%. m.p.: 226-227°C. FT-IR (KBr) ν_{\max} cm^{-1} : 3412 (N-H str.), 3078 (H-Ar str.), 1688 (C=O), 1679 (C=N str). $^1\text{H-NMR}$ (DMSO- d_6 , 300MHz) δ (ppm): 1.76 (s, 3H, CH₃), 5.76 (s, 1H, NH), 7.42-7.92 (m, 8H, Ar-H), 12.06 (s, 1H, NHC=O, D₂O exchangeable).

Synthesis of 2-(1H-benzo[d]imidazol-2-yl)-N-(1-(4-nitrophenyl) ethylidene) hydrazinecarboxamide (4q) Yield: 80%. m.p.: 226-228 °C. FT-IR (KBr) ν_{\max} cm^{-1} : 3410 (N-H str.), 3071 (H-Ar str.), 1690 (C=O), 1681 (C=N str); $^1\text{H-NMR}$ (DMSO- d_6 , 300MHz) δ (ppm): 1.75 (s, 3H, CH₃), 5.76 (s, 1H, NH), 7.41-7.89 (m, 8H, Ar-H), 12.02 (s, 1H, NHC=O, D₂O exchangeable).

Synthesis of N-(1-(2-aminophenyl) ethylidene)-2-(1H-benzo[d]imidazol-2-yl)hydrazinecarboxamide (4r) Yield: 76%. m.p.: 245-246°C. FT-IR (KBr) ν_{\max} cm^{-1} : 3502 (N-H str.), 3114 (H-Ar str.), 1842 (C=N str), 1695 (C=O); $^1\text{H-NMR}$ (DMSO- d_6 , 300MHz) δ (ppm): 1.86 (s, 3H, CH₃), 6.14 (s, 1H, NH), 7.28-7.52 (m, 8H, Ar-H); 12.32 (s, 1H, NHC=O, D₂O exchangeable).

Synthesis of N-(1-(2-aminophenyl) ethylidene)-2-(1H-benzo[d]imidazol-2-yl)hydrazinecarboxamide (4s) Yield: 79%. m.p.: 244-245°C. FT-IR (KBr) ν_{\max} cm^{-1} : 3500 (N-H str.), 3112 (H-Ar str.), 1844 (C=N str), 1698 (C=O). $^1\text{H-NMR}$ (DMSO- d_6 , 300MHz) δ (ppm): 1.87 (s, 3H, CH₃), 6.15 (s, 1H, NH), 7.30-7.53 (m, 8H, Ar-H); 12.28 (s, 1H, NHC=O, D₂O exchangeable).

Synthesis of (E)-2-(1H-benzo[d]imidazol-2-yl)-N-(1-o-tolylethylidene) hydrazinecarboxamide (4t) Yield: 74%. m.p.: 212-213°C. FT-IR (KBr) ν_{\max} cm^{-1} : 3476 (N-H str.), 3119 (H-Ar str.), 1742 (C=N str), 1632 (C=O). $^1\text{H-NMR}$ (DMSO- d_6 , 300MHz) δ (ppm): 2.16 (s, 3H, CH₃), 6.14 (s, 1H, NH), 7.22-7.72 (m, 8H, Ar-H); 12.12 (s, 1H, NHC=O, D₂O exchangeable).

Pharmacology:

Anticonvulsant Screening

A suspension of the test compounds in 0.5% carboxymethylcellulose was injected intraperitoneally into mice at doses of 30, 100, and 300 mg/kg. The MES and scPTZ models were used to assess the anticonvulsant efficacy of the investigated drugs. The Rota rod model was utilized to assess neurological toxicity while phenytoin and ethosuximide were utilized as standard medications for comparison. In order to measure the anticonvulsant activity of the compound, intraperitoneal (i.p.) injections of 30, 100, and 300 mg/kg body weight were given. The drug was delivered for 0.5 and 4 hours. Mice were subjected to electrical stimulation at 60 Hz and 50 mA for 0.2 seconds using ear-clip electrodes in order to induce maximal electroshock convulsions. An animal is regarded 'protected' from MES-induced seizures with cessation of the hind limb tonic extensor component of the seizure.^{13, 14}

After the test compounds were given to the animal for 30 minutes, 85 mg/kg of PTZ was dissolved in saline to create a solution, which was then given subcutaneously. The animals were kept in separate cages and watched for thirty minutes. The number of deaths and tonic-clonic convulsions that occurred were recorded.^{15, 16} Neurotoxicity (minimal motor impairment) was indicated as the median toxic dosage (TD50), and anticonvulsant activity was expressed as the

median effective dose (ED50). A computer program developed at the National Institute of Neurological Disorders and Stroke was used to determine the corresponding ED50 and TD50 values, 95% confidence intervals, slope of the regression line, and standard error of the slope based on the plot of this data.

Neurotoxicity Screening (NT)

The standardized Rotarod¹⁷ test was used to evaluate mild motor impairment in mice. A 3.2 cm diameter of Rotarod revolving at 6 rpm was used to evaluate each mouse. Intraperitoneal (i.p.) injections of the test drugs at dosages of 30, 100, and 300 mg/kg were administered to trained animals. Neurotoxicity was discovered by the inability of the animals to maintain equilibrium on the revolving rod for at least 1 minute in each of the four trials. This test serves as a reliable method for detecting subtle motor deficits generated by the test substances.

Estimation of Enzymes

The study dealt with estimating the levels of Serum Glutamate Oxaloacetate Transaminase (SGOT or AST) and Serum Glutamate Pyruvate Transaminase (SGPT or ALT), enzymes found in liver and heart cells, using Reitman and Frankel's method.^{18, 20} Increased SGOT and SGPT levels can suggest liver or heart damage, and their examination is critical in detecting illnesses such as alcoholic hepatitis, cirrhosis, and cardiac arrest. The study also assessed the activity of alkaline phosphatases, which are important liver health-related enzymes, in an alkaline environment. Standardized enzymatic assays are used to monitor liver function and associated disorders and guarantee precise findings.²¹

Estimation of Proteins

Proteins, as essential cellular macromolecules, are integral to diverse biological functions. In the realm of experimental research, measuring protein concentration is a versatile assay with broad applications. In the specific context of chronic liver diseases, protein determination holds particular significance as it furnishes valuable insights into the overall protein content in biological samples. In this study, the Biuret method^{22,26}, a well-established technique, was employed for accurately determining protein concentration. This method, often used for its reliability, involves the formation of a colored complex when copper ions react with peptide bonds in proteins, enabling precise quantification of protein levels.

Ethanol Potentiation Test

The Ethanol Potentiation Test employed in this experiment consisted of administering the test compound to mice, followed by an intraperitoneal injection of ethanol (2.5 g/kg) one hour later. The chosen ethanol dose was carefully selected to avoid inducing lateral positioning in control animals. Subsequently, the study assessed the number of animals in each group that exhibited lateral positioning after the administration of ethanol²³. This test aims to evaluate the potential modulation of ethanol-induced effects by the test compound, particularly focusing on observable behavioral responses.

Docking Studies

The crystal structure of the NMDA glutamate receptor in complex with Ifenprodil (PDB ID: 3QEL) was obtained from the Protein Data Bank (PDB) at <http://www.rcsb.org/pdb>. This structure served as the basis for conducting docking analysis, allowing for the exploration of the molecular interactions between the receptor and Ifenprodil, providing insights into their binding interactions at the atomic level.²⁴ The protein structure was corrected and minimized, solvent molecules were removed, and bond orders for both the ligand and protein were adjusted. Hydrogen atoms were added to the protein, and the entire structure was minimized using the OPLS2005 force field. The compound (**4e**) was corrected and optimized using the OPLS2005 force field in the Ligprep module of Schrödinger. For the docking study, the GLIDE 5.5 module of Schrödinger was employed. The 'Extra Precision' (XP) Glide algorithm was used to dock the ligand into the active site of the protein. The docked conformations were subsequently ranked based on the Glide score. The Glide score serves as an indicator of the binding affinity between the ligand and the receptor, with lower scores suggesting more favorable binding interactions. (Figure 2 and 3).

Results and Discussion

Chemistry

The synthesis of intermediate and target compounds was carried out following the synthetic protocol outlined in Scheme 1. H-benzo[d]imidazole-2-thiol (**1**) was prepared using a previously reported method. Subsequently, 2-hydrazinyl-1H-benzo[d]imidazole (**2**) was synthesized by treating compound (**1**) with hydrazine hydrate in methanol. Compound (**2**) was then condensed

with sodium cyanate and glacial acetic acid, resulting in the formation of 2-(1H-benzo[d]imidazol-2-yl) hydrazinecarboxamide (**3**). The target compounds (**4a-t**) were obtained through further condensation with respective aromatic aldehydes or ketones. The synthetic steps outlined in Scheme 1 detail the progression from the starting material to the intermediate and ultimately to the final target compounds. The assigned structures of the compounds were corroborated by a comprehensive analysis, including elemental analysis, infrared spectroscopy (IR), proton nuclear magnetic resonance ($^1\text{H-NMR}$), and mass spectrometry. The mass spectra (ESI-MS) analysis revealed the presence of peaks at definite m/z (mass-to-charge ratio) values consistent with the molecular formulas of the compounds. The elemental analysis results demonstrated a high level of accuracy, with deviations within $\pm 0.4\%$ of the theoretical values.

The title compounds were synthesized in four steps, following the synthetic protocol outlined in Scheme 1. In the initial step, 1 H-benzo[d]imidazole-2-thiol (**1**) was synthesized by reacting *o*-phenylenediamine (1 mmol) in 10 mL of ethanol with potassium hydroxide (1 mmol) and carbon disulfide (1 mmol). The IR spectra of compound (**1**) exhibited characteristic stretching bands at 2634 cm^{-1} , corresponding to S-H, and at 3395 cm^{-1} , attributed to N-H in the benzimidazole moiety. In the $^1\text{H-NMR}$ spectra, a singlet appeared at δ 12.31, which could be attributed to the presence of S-H, while another singlet at around δ 10.93 indicated the N-H in the benzimidazole ring. These spectroscopic features provide valuable information about the functional groups present in compound (**1**), supporting its structural characterization. ^{13}C NMR spectra displayed a chemical shift at around δ 151.93, attributed to (N=C-N) of the benzimidazole ring. Additionally, peaks at 130.72, 130.41, 127.68, 125.34, 116.58, and 115.91 were observed, indicating the presence of aromatic carbon in the compound. In the second step, 2-hydrazinyl-1H-benzo[d]imidazole (**2**) was synthesized by reacting compound (**1**) (1 mmol) with hydrazine hydrate (1 mmol) in methanol (10 mL). This step in the synthetic protocol contributes to the formation of the desired hydrazinyl derivative. The compound (**2**) showed differences in R_f value and melting point observed for compound (**2**) compared to the starting compound (**1**). The IR spectra of compound (**2**) revealed characteristic stretching bands at 3464 and 3024 cm^{-1} , corresponding to N-H and C-H groups. These bands provide additional evidence supporting the presence of specific functional groups in the synthesized compound. In $^1\text{H-NMR}$ spectra the singlet appeared at δ 6.9 could be accounted for the presence of N-H and it is confirm by D_2O

exchange. ^{13}C NMR spectra exhibited a chemical shift at approximately δ 152.3, which corresponds to the N=C-N group in the benzimidazole ring. Additionally, peaks at 131.63, 129.51, 129.17, 123.81, 115.17, and 114.95 were observed, indicating the presence of benzimidazole aromatic carbon. The mass spectrum of compound (**2**) displayed a molecular ion peak at m/z 148, which is consistent with the molecular formula $\text{C}_7\text{H}_8\text{N}_4$.

In the third step of the synthesis, compound (**2**) was treated with sodium cyanate (5 mL) in the presence of a minimum quantity of water and glacial acetic acid (5 mL) to form 2-(1H-benzo[d]imidazol-2-yl)hydrazinecarboxamide (**3**). The IR spectra of compound (**3**) displayed characteristic peaks at around 3505 and 3028 cm^{-1} , corresponding to N-H and Ar-H groups, respectively. Another characteristic peak appeared at 1623 cm^{-1} indicating the presence of C=O of carboxamide. In ^1H -NMR spectra, appeared a singlet at around δ 6.78 indicative of N-H and disappeared by addition of D_2O as confirmation for this group. The characteristic singlet appeared in ^1H NMR at δ 9.56 indicative the presence of $\text{NHC}=\text{O}$ of carboxamide group. Chemical shift in ^{13}C NMR at around δ 163.73 indicated C=O of carboxamide and at δ 155.61 due to N=C-N group indicating the formation of benzimidazole ring. In the fourth step, substituted (1H-benzo[d]imidazol-2-yl)-N-benzylidenehydrazinecarboxamides (**4a-t**) were synthesized by reacting compound **3** (1 mmol) with various aromatic aldehydes and ketones (0.112 mmol) in the presence of glacial acetic acid (5 mL) and ethanol (10 mL). The completion of the reaction was verified by a single-spot TLC using solvent systems such as toluene : ethyl acetate : formic acid (5:4:1) or benzene : acetone (9:1). The observed differences in R_f values and melting points for the title compounds (**4a-t**) compared to the starting compound (**3**). The general IR spectra of the compounds exhibited characteristic bands at around 3489 and 3020 cm^{-1} for N-H and C-H (Ar-H) group.

In the ^1H -NMR spectra, a singlet appeared at around δ 6.75, indicating the presence of N-H in the benzimidazole ring. The confirmation of this N-H group was further supported by its disappearance upon the addition of D_2O . The presence of C=O and N=C-N groups was confirmed by the appearance of characteristic band appeared at around 1685 and 1598 cm^{-1} in IR spectra. The ^{13}C NMR spectra showed the peaks at around δ 169.51 and 157.63 due to C=O and =CH. In ^1H -NMR spectra, two singlet appeared at around δ 6.75 and 12.56 could be accounted for N-H (benzimidazole ring) and C-H (=C-H), respectively. The signals were appeared in ^{13}C

NMR spectra at around δ 153.46 (N=C-N), 132.53, 131.62, 129.47, 128.72, 128.21, 125.83, 125.17, 123.23, 120.41, 118.54, 117.61 and 112.93 due to aromatic carbon.

Pharmacological assay (in-vivo anticonvulsant activity)

According to the criteria of the Anticonvulsant Screening Program²⁵ (ASP) of the National Institute of Neurological Disorders and Stroke (NINDS) for the screening of substances for putative anticonvulsant capabilities and supplying critical information about how effectively they function to reduce seizures. The Subcutaneous Pentylentetrazole (scPTZ) model and the Maximal Electroshock Seizure (MES) model were utilized for the screening. Intraperitoneal (i.p.) injections of the compounds at dosages of 30, 100, and 300 mg/kg body weight were employed. The neurotoxicity studies, specifically the determination of minimum motor impairment, were conducted with the rotorod approach. Table 2.

In Phase I, multiple drugs (**4e**, **4g**, **4h**, **4i**, **4o**, **4p**, and **4q**) were found as active against the MES model at a dose level of 30 mg/kg within a 0.5-hour time interval. Notably, compounds (**4e**, **4h**) and (**4p**) displayed persistent anticonvulsant activity even after 4.0 hours at the same dose, demonstrating their efficacy in reducing seizure propagation at a relatively low dosage. At a dosage of 100 mg/kg during the 0.5-hour time period, chemicals (**4c**, **4d**, **4m**, **4n**, **4r**) and (**4t**) demonstrated moderate protection against the MES model. The majority of the drugs displayed anticonvulsant activity during the 0.5-hour timeframe suggesting a quick onset of action. In the chemo shock experiment, many drugs (**4d**, **4e**, **4g**, **4h**, **4o**, and **4q**) displayed efficacy at a dose of 100 mg/kg during the first 0.5 hours. Notably, compounds (**4e**) and (**4p**) continued their efficacy even after 4.0 hours at the same dose. Compound (**4c**, **4i**) and (**4j**) demonstrated effect at a higher dose of 300 mg/kg within the first 0.5 hours. Compounds (**4o**) and (**4q**) maintained their action after 4.0 hours at both the tested doses (100 mg/kg and 300 mg/kg). In neurotoxic investigations employing rotorod and ethanol potentiation testing. Even at the maximum dose of 300 mg/kg, compounds (**4b**, **4c**, **4e**, **4g**, **4h**, **4o**, **4p**, **4q**), and (**4r**) did not showed neurotoxicity, as

demonstrated by the lack of moderate motor impairment. Compared to phenytoin, the compounds (**4a**, **4d**, **4f**, **4i**, **4j**), and (**4m**) were demonstrated to be less neurotoxic. The chemicals (4f, 4k, 4l, 4n, 4s) and (4t) were discovered to be neurotoxic in compared to phenytoin. The ethanol potentiation test, required generating a lateral posture in the animals following the injection of ethanol and the findings of the test reveal that chemicals (**4h**) and 4m demonstrated an interaction with ethanol, potentiating its effects. On the other hand, chemicals (**4d**, **4e**, **4g**, **4i**, **4n**, **4o**, **4p**, **4q**, **4r**) and (4t) did not show an interaction with ethanol and results summarized in Table 2.

The Phase-II anticonvulsant screening of compounds (**4e**) and (**4h**) is an essential stage for evaluating their potential therapeutic efficacy. The assessment of essential pharmacological characteristics, such as the ED50 (median effective dose) and neurotoxicity TD50 (median toxic dose), is important for assessing their anticonvulsant effectiveness and safety profile.

Both compounds, (**4e**) and (**4h**) displayed activity equivalent to standard medications is a hopeful indicator of their potential as anticonvulsant agents. The better protective index (TD50 / ED50) obtained for both compounds in contrast to standard medicines further highlights their positive safety margin. The inclusion of multiple electron-withdrawing and electron-releasing groups at different places on the phenyl ring allows for a sophisticated examination of Structure-Activity Relationship (SAR). SAR studies are useful in understanding how structural alterations influence the biological activity of substances. The specific example of compound (**4e**) with a chloro group (-Cl) in the meta position of the phenyl ring, shows this relationship. The comparison of compound (4e) with proven medications like Phenytoin and Carbamazepine, as provided in Table 3, further underlines its advantages in terms of both activity and safety. Compound (4e) is a good candidate for additional research as an anticonvulsant medication since this shows that it may have the ability to perform better than the market standards as of yet.

In conclusion, the thorough pharmacological assessment, which includes ED50, TD50, and SAR studies, offers a strong basis for the development of compounds' anticonvulsant potential. Compound (4e) in particular merits for further research and development of these compounds as possible anticonvulsant agents with enhanced efficacy and safety profiles.

Enzyme and Protein estimation

The evaluation of hepatotoxic effects of compounds (**4e**) and (**4h**) involved a comprehensive analysis of liver enzymes, providing valuable insights into their potential impact on hepatic function. Alkaline phosphatase, Serum Glutamate Oxaloacetate Transaminase (SGOT), and Serum Glutamate Pyruvate Transaminase (SGPT) are crucial biomarkers that reflect liver health. The utilization of these markers in the assessment of compound-induced hepatotoxicity is a standard practice in pharmacological research. For compound (**4e**) the non-significant change in enzyme levels compared to the control group, denoted by $P < 0.01$, is a statistically robust observation. This implies that, at the tested concentrations, compound 4e did not induce any significant alterations in alkaline phosphatase, SGOT, or SGPT levels. Such stability in enzyme levels suggests a lack of hepatotoxic effects associated with compound (**4e**).

On the other hand, the moderate increase in alkaline phosphatase and SGPT levels with compound 4h, accompanied by a significant rise in SGOT levels ($P < 0.05$), demands closer scrutiny. While these changes may be indicative of some hepatic impact, the absence of significant alterations in other parameters suggests a nuanced effect on liver enzymes. The intricacies of these changes need to be considered in the broader context of hepatic function.

The subsequent assessment of albumin and globulin levels provides additional depth to the analysis. Albumin and globulin are integral proteins synthesized by the liver, and their levels serve as crucial indicators of hepatic performance. The significant increase in blood albumin levels after the administration of compounds (**4e**) and (**4h**) is a noteworthy finding. Elevated albumin levels are often associated with improved liver function, suggesting a positive impact of the compounds on hepatic synthesis processes.

It's important to note that while changes in liver enzyme levels can indicate potential hepatotoxicity, a comprehensive evaluation, including histopathological examinations and long-term studies, is essential for a thorough understanding of the compounds' safety profile. Additionally, the observed increase in albumin levels hints at potential therapeutic benefits, but further investigations are warranted to elucidate the underlying mechanisms and ensure the overall safety and efficacy of the compounds.

Docking Studies

Using the Glide 5.0 module of the Schrödinger Maestro Package to predict the anticonvulsant activity of the synthesized compounds (**4a-t**) and the obtained glide scores are shown in Table 2.

Compound (**4e**) has shown maximum affinity towards 3QEL. The docked poses of 3QEL inhibitors of compound (**4e**) in the active sites are shown in Figure 2. The GLIDE score was found to be -9.35kcal/mol and has shown maximum affinity towards PBP. Docking study showed that compound (**4e**) makes hydrophobic interaction with the amino acids via ALA107, TYR109, GLN110, ILE111, PHE114, LYS131, HIS134, LEU135, ILE138, THR233 etc, which constitutes the empty hydrophobic space of the protein. Furthermore NH of benzimidazole and NH adjacent to the carbonyl group make two Hydrogen bonds with the polar amino acid residue SER 132 (Figure 3). The docking study of compound (**4e**) was found to be in accordance with the previous study as shown by *Karkas et al*²⁴, where they had shown the mechanism of inhibition of NMDA glutamate receptor by Ifenprodil. According to the author, the interaction of Ifenprodil with the empty hydrophobic space amino acid residue via ALA75, ILE82, TYR109, PHE114, LEU135, PHE176, and PRO177 and polar interaction with SER132, GLN110, ASP 236 is critical in mediating Ifenprodil induced inhibition of NMDA glutamate receptor.

Results:

After looking of active pharmacophore modeling and successfully designed and synthesized a series of new compounds, specifically 1H-benzo[d]imidazol-2-yl)-N-benzylidene hydrazine carboxamides (**4a-t**). Utilizing computational approaches like pharmacophore modeling to guide the design of new chemical entities is a powerful strategy in drug discovery. The synthesized compounds were evaluated for their in-vivo anticonvulsant activity, and the results suggest that compounds with the benzimidazole moiety and specific substituents (Cl and NO₂ groups) at the hydrophobic aryl ring exhibited highly potent activity. The compounds with substituents OCH₃, OH, and NH₂ on the benzimidazole moiety and an unsubstituted hydrophobic aryl ring exhibit moderate to decreased activity provides valuable information about the impact of specific functional groups on the overall pharmacological properties of the compounds. The identification of compounds (**4e**) and (**4h**) as particularly promising, with excellent activity and higher safety compared to marketed drugs such as carbamazepine, phenytoin, and ifenprodil, is a significant achievement in your research. Performing molecular docking studies using the Maestro 9.0 program to investigate the binding mode of compound 4e into the binding sites of the NMDA Glutamate receptor (PDB Id: 3QEL) is a valuable computational approach. Insight of these points, pharmacological evaluations, molecular docking studies, and structure-activity

relationship analyses highlight The compelling properties exhibited by compound (4e) position it as an auspicious candidate for in-depth investigations as a potential novel anticonvulsant agent

Acknowledgements

The authors would like to extend their appreciation to the Dean of Research at Singhania University, Rajasthan (India), for generously providing the facilities required for this research. Special thanks are also directed to IIT New Delhi for the provision of spectral data.

Conflict of Interest: No conflicts of interest were declared by the authors for this study.

References

1. Xianran He, Zhong M, Zhang T, Wu W, Wu Z, Yang J, Yuling X, Pan Y, Qiu G, Hu X. Synthesis and anticonvulsant activity of N-3-arylamide substituted 5,5-cyclopropanespirohydantoin derivatives. *Eur. J. Med. Chem.*, 2010; 45: 5870-5877.
2. Kulandasamy R, Adhikari A V, Stables J P. A new class of anticonvulsants possessing 6 Hz activity: 3,4-Dialkyloxy thiophene bishydrazones. *Eur. J. Med. Chem.*, 2009; 44: 3672–3679.
3. Vasil'ev P M, Kalitin KY, Spasov A A, Grechko OY, Poroikov V V, Filimonov D A, Anisimova V A. Prediction and study of anticonvulsant properties of benzimidazole derivatives. *Pharm. Chem. J.* 2017; 50: 775–780.
4. Argirova M A, Georgieva M K, Hristova-Avakumova N G, Vuchev D I, Popova-Daskalova, G V, Anichina K K, Yancheva D Y. New 1H-benzimidazole-2-yl hydrazones with combined antiparasitic and antioxidant activity. *RSC. Adv.* 2021; 11: 39848–39868.
5. Zalaru C, Dumitrascu F, Draghici C, Tarcomnicu I, Marinescu M, Nitulescu G M, Tatia R, Moldovan L, Popa M, Chifiriuc M C. New Pyrazolo-Benzimidazole Mannich Bases with Antimicrobial and Antibiofilm Activities. *Antibiotics.* 2022; 11: 1094.
6. Chen M, Su S, Zhou Q, Tang X, Liu T, Peng F, He M, Luo H, Xue W. Antibacterial and antiviral activities and action mechanism of flavonoid derivatives with a benzimidazole moiety. *J Saudi Chem Soc.* 2021; 25: 101194.

7. Moharana A K, Dash R N, Mahanandia N C, Subudhi B B. Synthesis and anti-inflammatory activity evaluation of some benzimidazole derivatives. *Pharm. Chem. J.* 2022, 56: 1070–1074.
8. Pandeya S N, Ponnilarasan I, Pandey A, Lakhan R, Stables J P. Evaluation of *p*-nitrophenyl substituted semicarbazones for anticonvulsant properties. *Pharmazie* 1999; 54: 923-925.
9. Wong M G, Defina J A, Andrews P R. Conformational analysis of clinically active anticonvulsant drugs. *J. Med. Chem.* 1986; 29: 562-572.
10. Pandeya S N, Yogeeswari P, Stables J P. Synthesis and anticonvulsant activity of 4-bromophenyl substituted aryl semicarbazones. *Eur. J. Med. Chem.*, 2000; 35: 879–886.
11. Wang M L and Liu C Y. Reaction of *o*-phenylene diamine and carbon disulfide by potassium hydroxide at higher temperature. *J. Taiwan Inst. Chem. Eng.* 2009; 40: 586–591.
12. Wang M L and Liu B L. Synthesis of 2-mercaptobenzimidazole from the reaction of *o*-phenylene diamine and carbon disulfide in the presence of potassium hydroxide. *J. Chinese Inst. Chem. Eng.* 2007; 38: 161–167.
13. Krall R L, Penry J K, White B G, Kupferberg H J, Swinyard E A. Antiepileptic drug development II. Anticonvulsant drug screening. *Epilepsia.* 1978; 19: 409–428.
14. Swinyard E A, Woodhead J H, White H S, Franklin M R. *Antiepileptic Drugs*. Raven Press New York. 1989: 85-102.
15. White H S, Johnson M, Wolf H H, Kupferberg H J. The early identification of anticonvulsant activity: role of the maximal electroshock and subcutaneous pentylenetetrazol seizure models. *Ital. J. Neurol. Sci.* 1995: 16:73-77.
16. Poter R J, Cereghino J J, Gladding G D, Hessie B J, Kupferberg H J, Scoville B, *Cleve Clin Q. Antiepileptic Drug Development Program.* 1984; 51: 293-305.
17. Dunham N W and Miya T A. A note on a simple apparatus for detecting neurological deficit in rats and mice *J. Am. Pharm. Assoc. Sci.* 1957; 46: 206-212.
18. Reitman S, Frankel S A. A colorimetric method for the determination of serum glutamic oxalacetic and glutamic pyruvic transaminases. *Am. J. Clin. Pathol.* 1957; 28: 56-62.
19. Tietz N. *Fundamentals of Clinical Chemistry*, W. B. Saunders Company, Philadelphia. U.S.A, 1970: 447-449.

20. King E J, Armstrong A R. A convenient method for determining serum and bile phosphatase activity. *Can. Med. Assoc. J.* 1934; 31: 376-381.
21. Reinhold J G and Reiner M. *Standard Methods in Clinical Chemistry* Academic Press New York. 1953; 88-90.
22. Varley H. *Practical Clinical Biochemistry*, CBS Publishers and Distributors, New Delhi, 1988: 236-238.
23. Clerici F, Pocar D. Synthesis of 2-amino-5-sulfanyl-1,3,4-thiadiazole derivatives and evaluation of their antidepressant and anxiolytic activity. *J. Med. Chem.* 2001; 44: 931–936.
24. Karakas E, Simorowski N, Furukawa H. Subunit Arrangement and Phenylethanolamine Binding in GluN1/GluN2B NMDA Receptors. *Nature* 2012; 475: 249-253.
25. Anticonvulsant Screening Project: Antiepileptic Drug Development Program National Inst Health DHEW Publication (NIH) (US) 1978: 78–1093.
26. Mistry, M., Shah, D., Pathak, P., & Zamani, A. S. (2013, March). Ontologies: Need, usage and attainment of health care system. In 2013 International Conference on Intelligent Systems and Signal Processing (ISSP) (pp. 381-386). IEEE.
27. Mengash, Hanan Abdullah, Mohammad Alamgeer, Mashaal Maashi, Mahmoud Othman, Manar Ahmed Hamza, Sara Saadeldeen Ibrahim, Abu Sarwar Zamani, and Ishfaq Yaseen. "Leveraging marine predators algorithm with deep learning for lung and colon cancer diagnosis." *Cancers* 15, no. 5 (2023): 1591.
28. Jasti, V. Durga Prasad, Abu Sarwar Zamani, K. Arumugam, Mohd Naved, Harikumar Pallathadka, F. Sammy, Abhishek Raghuvanshi, and Karthikeyan Kaliyaperumal. "Computational technique based on machine learning and image processing for medical image analysis of breast cancer diagnosis." *Security and communication networks* 2022, no. 1 (2022): 1918379.

Table 1: Physicochemical parameters and substitution (R and R¹) of the title compounds (**4a–t**).

Compd	R	R ¹	Mol. Formula ^a	Log P Experimental ^b	R _f value ^c	Elemental Analyses		
						% Found (Calculated) ^d		
						C	H	N
4a.	H	H	C ₁₅ H ₁₃ N ₅ O	2.80	0.66	64.51 (65.54)	4.69 (4.6)	25.10 (25.13)
4b.	H	2-OH	C ₁₅ H ₁₃ N ₅ O ₂	2.45	0.67	61.01 (61.05)	4.44 (4.40)	23.72 (23.70)
4c.	H	4-OH	C ₁₅ H ₁₃ N ₅ O ₂	2.42	0.59	61.03 (61.05)	4.42 (4.4)	23.71 (23.70)
4d.	H	2-Cl	C ₁₅ H ₁₂ ClN ₅ O	3.35	0.56	57.42 (57.71)	3.86 (3.5)	22.32 (22.62)
4e.	H	3-Cl	C ₁₅ H ₁₂ ClN ₅ O	3.33	0.52	57.38 (57.71)	3.89 (3.5)	22.29 (22.60)
4f.	H	4-Cl	C ₁₅ H ₁₂ ClN ₅ O	3.36	0.54	57.44 (57.71)	3.82 (3.5)	22.35 (22.61)
4g.	H	2-NO ₂	C ₁₅ H ₁₃ N ₅ O	2.50	0.71	55.55 (55.22)	3.73 (3.7)	29.91 (29.67)
4h.	H	4-NO ₂	C ₁₅ H ₁₃ N ₅ O	2.53	0.65	55.52 (55.22)	3.76 (3.7)	29.89 (29.65)
4i.	H	2-OCH ₃	C ₁₆ H ₁₅ N ₅ O ₂	2.67	0.55	62.13 (62.38)	4.89 (4.5)	22.64 (22.91)
4j.	H	3,4- (OCH ₃) ₂	C ₁₅ H ₁₃ N ₅ O	2.54	0.59	60.13 (60.38)	5.05 (5.1)	20.64 (20.95)
4k.	H	4- N(CH ₃) ₂	C ₁₇ H ₁₈ N ₆ O	3.54	0.49	67.22 (67.52)	4.23 (4.4)	19.60 (19.25)
4l.	CH 3	H	C ₁₆ H ₁₅ N ₅ O	2.36	0.64	65.52 (66.22)	5.15 (5.4)	23.88 (23.62)
4m.	CH 3	2-OH	C ₁₆ H ₁₅ N ₅ O ₂	1.95	0.66	62.13 (62.42)	4.89 (5.2)	22.64 (22.92)
4n.	CH 3	4-OH	C ₁₆ H ₁₅ N ₅ O ₂	1.97	0.57	62.11 (62.42)	4.92 (5.2)	22.69 (22.90)
4o.	CH 3	2-Cl	C ₁₆ H ₁₄ ClN ₅ O	2.90	0.56	58.63 (58.26)	4.31 (4.6)	21.37 (21.54)
4p.	CH 3	3-Cl	C ₁₆ H ₁₄ ClN ₅ O	2.92	0.54	58.58 (58.26)	4.28 (4.6)	21.29 (21.58)
4q.	CH 3	4-Cl	C ₁₆ H ₁₄ ClN ₅ O	2.94	0.61	58.60 (58.26)	4.36 (4.6)	21.32 (21.56)
4r.	CH 3	3-NO ₂	C ₁₆ H ₁₄ N ₆ O ₃	2.64	0.62	56.80 (57.06)	4.17 (4.4)	24.84 (24.58)

4s.	CH 3	3-NH ₂	C ₁₆ H ₁₆ N ₆ O	1.56	0.53	62.32 (61.94)	5.23 (5.6)	27.26 (27.64)
4t.	CH 3	4-NH ₂	C ₁₆ H ₁₆ N ₆ O	1.55	0.54	62.35 (61.94)	5.20 (5.6)	27.19 (27.62)

^aSolvent of crystallization–Ethanol.^bLog P was determined by octanol:phosphate buffer method; CLog P was calculated using software Chem Bio Office 11.0.^cSolvent system- Benzene : Acetone (8:2) and Toluene: Ethyl acetate : Formic acid (5:4:1).^dElemental analysis for C, H and N were within ± 0.4 % of the theoretical value.

Table 2: Anticonvulsant activity and minimal motor impairment of the test compounds (**4a–t**).

Compd.	Intraperitoneal injection in mice ^a							
	MES screen		scPTZ screen		Neurotoxicity screen			Glide Score ^c
	0.5 h	4.0 h	0.5 h	4.0 h	0.5 h	4.0 h	Ethanol Potentiation test	
4a	300	- ^b	-	-	-	-	300	-7.01686
4b	-	300	-	-	-	-	x	-7.74545
4c	100	-	300	300	-	-	x	-7.76907
4d	100	100	100	-	300	-	x	-7.44912
4e	30	30	100	100	-	-	-	-9.35036
4f	300	300	-	-	100	300	-	-7.91244
4g	30	100	100	-	-	-	x	-6.95304
4h	30	30	100	-	-	-	-	-8.84097
4i	30	100	300	-	-	300	+	-8.032614
4j	-	300	300	-	300	300	-	-7.54406
4k	300	-	-	-	-	100	x	-7.45405
4l	-	300	-	300	-	100	x	-7.60887
4m	100	100	-	-	-	300	+	-7.63901

4n	100	300	-	-	-	100	-7.01687
4o	30	100	100	300	-	-	-7.15993
4p	30	30	-	100	-	-	-9.13762
4q	30	100	100	300	-	-	-7.99154
4r	100	100	-	-	-	-	-8.7718
4s	300	300	-	-	-	100	-7.28203
4t	100	300	-	-	-	100	-8.91186
Phenytoin	30	30	-	-	100	100	-8.39400
CBZ	30	100	100	100	-	-	-7.39553

Number of animals in each group (n) = 6; Dose of 30, 100 and 300 mg/kg were administered i.p. The figures indicate the minimum dose whereby bioactivity was demonstrated in half or more mice. The - indicates an absence of activity at maximum dose administered (300 mg/kg). The X indicates not tested. ^bEthanol Potentiation test; The + indicates half or more animals passed the test while - indicates failed.

Table 3. Phase II quantitative obtained anticonvulsant data in mice.

Compds.	ED ₅₀ ^a		TD ₅₀ ^b	PI ^c	
	MES	scPTZ		MES	scPTZ
4e	19.3 (16.9-21.4)	79.2 (69.3-88.6)	684.7 (615.5-761.6)	35.4	8.6
4h	25.2 (22.6-27.5) ^d	75.6 (64.4-85.5)	464.8 (417.8-517.1)	18.4	6.1
Phenytoin	9.5 (8.1-10.4)	>300	65.5 (52.5-72.9)	6.9	<0.22
Carbamazepine	8.8 (5.5-14.1)	>100	71.6 (45.9-135)	6.4	0<.22

Number of animals used: 10; solvent used: polyethylene glycol (0.1 ml, i.p.)

^aDose in mg/kg body weight.

^bMinimal toxicity which was determined by rotorod test 30 min after the test drug was administered.

^c PI = Protective index (TD₅₀/ED₅₀).

^dData in parentheses are the 95% confidence limits.

Table 4: Enzyme estimation of the selected test compounds.

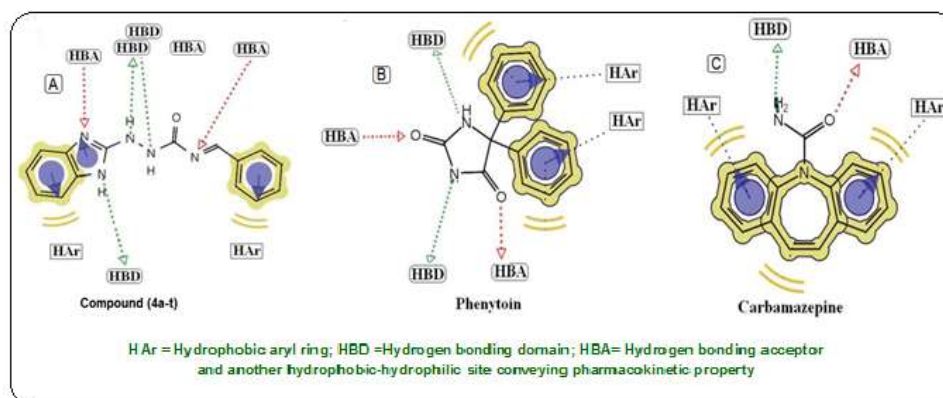
Treatment	Alkaline phosphatase \pm SEM	SGOT \pm SEM	SGPT \pm SEM
Control	16.5 \pm 0.543	153.06 \pm 0.958	23.88 \pm 0.663
4e	26.91 \pm 0.729**	182.88 \pm 1.934*	38.19 \pm 0.609**
4h	34.78 \pm 0.933*	215 \pm 1.650	52.80 \pm 08481*

*P < 0.05; **P < 0.01. Results are given as mean total protein level \pm SEM and was calculated by dunnett's multiple comparison tests.

Table 5. Protein estimation of selected test compounds.

Treatment	Albumin (g/100ml) \pm SEM	Globulin (g/100ml) \pm SEM	Total protein (g/100ml) \pm SEM	Albumin/Globulin (g/100ml) \pm SEM
Control	1.35 \pm 0.037	0.59 \pm 0.014	1.94 \pm 0.015	2.28 \pm 0.082
4e	1.62 \pm 0.049	0.61 \pm 0.130**	2.23 \pm 0.104	2.65 \pm 0.106
4h	1.75 \pm 0.407	0.72 \pm 0.068	2.47 \pm 0.025*	2.43 \pm 0.036*

*P < 0.05; **P < 0.01. The mean level of Albumin/ Globulin \pm SEM were calculated using ANOVA followed by dunnett's multiple comparison test.

**Figure 1:** Pharmacophore modeling of title compounds (4a-t) with the reference drugs (Phenytoin & Carbamazepine).

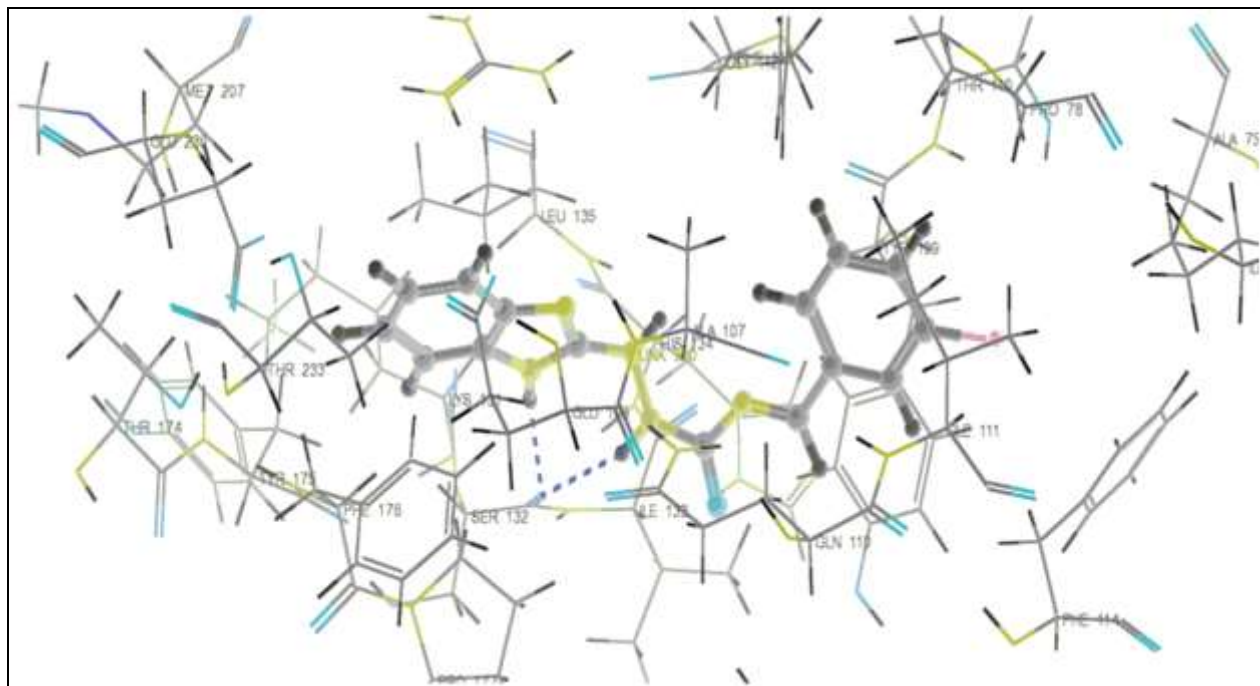


Figure 2: Docked poses of crystal structure of NMDA Glutamate receptor (PDB Id: 3QEL) in complex with Ifenprodil (active sites for compound 4e).

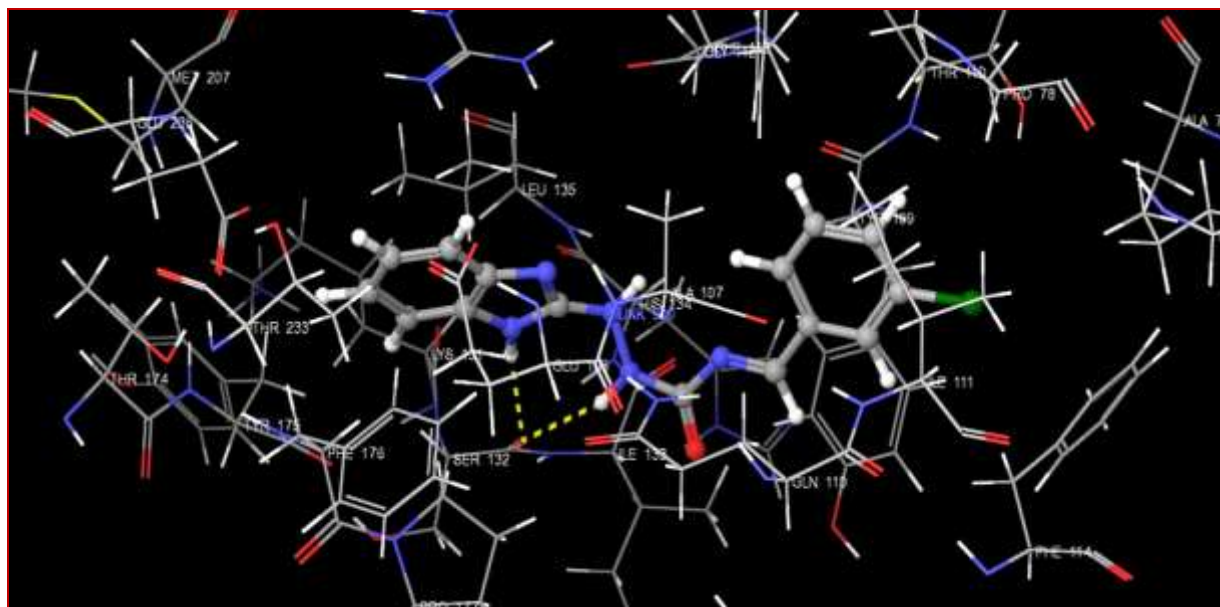
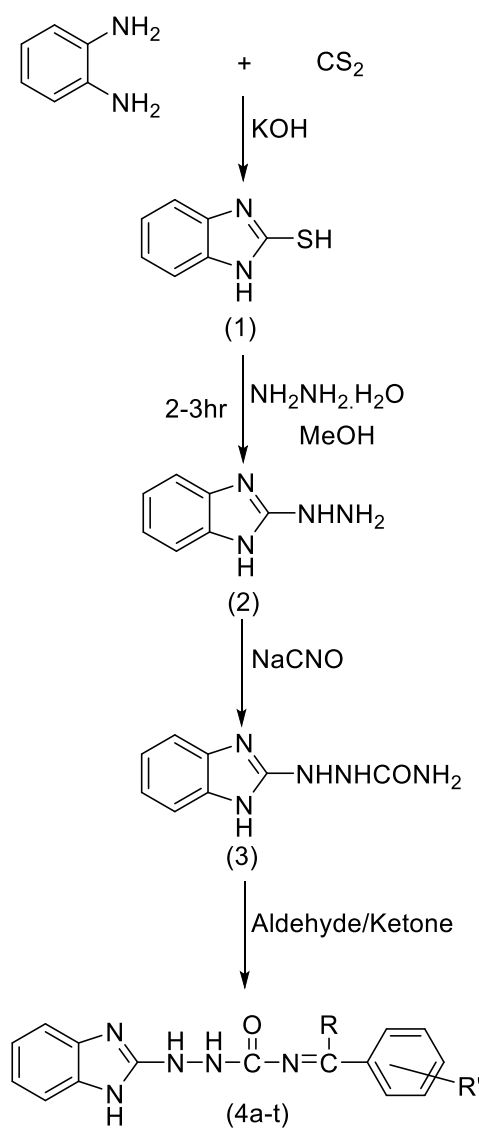


Figure 3. Binding patterns of compound **4e** into the binding sites of NMDA glutamate receptor (PDB ID: 3QEL) showing hydrogen bond (yellow dotted lines) with SER 132 (1.72 Å) and hydrophobic interaction with the amino acids via ALA107, TYR109, GLN110, ILE111, PHE114, LYS131, HIS134, LEU135, ILE138, THR233.



Scheme 1. Reagent and conditions: (1) EtOH, Reflux, 12-14h
 (2) NH2.NH2.H2O, Reflux, 4-5 h (3) Glacial- CH3COOH (4a-t) EtOH, Glacial CH3COOH, Aldehyde or Ketones, Reflux, 5-6h.